SSRG International Journal of Electrical and Electronics Engineering
ISSN: 2348-8379/ https://doi.org/10.14445/23488379/IJEEE-V11I11P102

Volume 11 Issue 11, 12-22, November 2024

Original Article

A New MPPT for PV Array under Uniform Irradiation Using Exponential Scanning Technique

A. Arjun[1*], P. Selvam[1]

[1]*Department of Electrical and Electronics Engineering, Vinayaka Mission's Kirupananda Variyar Engineering College, Vinayaka Mission's Research Foundation (Deemed to be University), Tamilnadu, India.*

[*]*Corresponding Author : arrjun01@gmail.com*

Received: 02 September 2024 Revised: 02 October 2024 Accepted: 01 November 2024 Published: 30 November 2024

Abstract - *There has been a huge exploration since the invention of PV cells to find new techniques to efficiently fit the PV array for a particular application. Each technique has its own way of effectively extracting power from the PV source. In any way, all the techniques strive for faster convergence to Maximum Power Point (MPP) under static and dynamic irradiation conditions. Simplicity, accuracy and rapidity are the main aims of developing new techniques. In this paper a method was devised in a simple manner to reach MPP faster with excellent accuracy. The method was contemplated by focusing only on the PV characteristics' power zone and applying an interval in the said region. An exponential scanning algorithm is proposed, which makes the interval shrink sequentially in a self-adaptive fashion at each iteration by applying search conditions and finally reaches the MPP. The interval selection is also explained, and its practical determination requires only the data contained in the PV module's datasheet. Computer simulations and experimental evaluation confirm the effectiveness of the presented technique. The convergence to the MPP is faster, and the efficiency obtained in simulations and experimental evaluation is more than 99%.*

Keywords - *Exponential scanning algorithm, Forward and Reverse scanning, Maximum Power Point Tracking (MPPT), Power zone, Self-adaptive tracking, Uniform irradiation.*

1. Introduction

Due to the non-linear characteristic behavior of a PV array, it is inevitable that the PV array will be matched with the load to extract maximum power from the PV array under all environmental conditions. Usually, the matching is performed by connecting a switching converter between the PV source and the load and controlling the converter using an appropriate algorithm to extract maximum power from the PV source. The controlling algorithm used to do the task is termed the Maximum Power Point Tracking (MPPT) algorithm. At present, there are diversified techniques to track the MPP, which can be classified into different categories. Of them, the Perturb & Observe (P&O) Technique, Incremental Conductance Technique (INC) and their derivatives are the most popular.

The conventional P&O, INC and their derivatives, if looked into closely, shall be considered as scan and search algorithms, where the scanning over the possible or favorable region is based on certain algorithms and the search is based on certain conditions and constraints. In the case of P&O, the scanning is over the entire voltage region by the algorithm as expressed by, $V_n=V_{n-1}+\Delta V$ whereas the search is based on the comparison of powers between two iterations as given by, $P_n<P_{n-1}$ V $P_n>_{Pn-1}$where n represents n^{th} iteration throughout this paper, and ΔV is the perturbation size in voltage level. If ΔV it is positive, the scanning is in the forward direction (voltage increases) and is in the reverse direction (voltage decreases) when it is negative.

In the case of INC, the scanning procedure is the same; however the search is based on the condition given by [1] dI/dV=-I/V [1]. Though INC uses a different search condition, it is considered a special form of P&O [2]. Also, to have similar MPPT loop dynamics in INC like that of P&O, an equivalent INC method is proposed [3], where the search condition and the scan algorithm are modified, in which a scaling factor is multiplied with the discrete form of dP/dV the scanning algorithm.

An improved version of INC is proposed [4], wherein the tracking accuracy is increased by introducing two-step sizes, and a larger step size is used when the operating point is far away from the MPP; otherwise, a smaller step size is used. The scanning is performed by modifying the duty cycle, and the search condition is similar to that of INC. The distance of the operating point is determined by comparing the value of the ratio of change in power to change in voltage with a threshold

value. In [5], H. Abouadane et al. have proposed a derivative of P&O wherein the scanning is similar to the conventional P&O, but the search is based on a comparison of powers in three successive neighborhood operating points, P_n, P_{n-1}, P_{n-2} to decide the direction of travel to reach the MPP faster.

In another derivative of the P&O method [6], the search conditions are similar to the conventional P&O; however, in the scanning algorithm, a constant momentum (scale factor) is multiplied with the previous perturbation size, which is then added to a fixed step size to determine the current perturbation size.

A method for MPPT under rapidly changing irradiation is proposed [7] in which the perturbation parameter (voltage or current) is decided based on the location of the operating point either to the left or right side of the MPP. If $dP/dV>0$ perturbation of current is used and if $dP/dV<0$ then perturbation of voltage is used. The scanning is performed by modulating the perturbation parameter with a fixed size, and the search condition is based on the reference generated by the controller to satisfy $dP/dV=0$.

There are various adaptive MPPT methods with variable step sizes available in the literature. In one of the methods of such an adaptive MPPT [8], the search condition is based on $V_{oc}/I_{sc}>V_n/I_n$ and the scanning algorithm varies the duty cycle by modifying the previous duty cycle by adding a product of $(V_{oc}/I_{sc}-V_n/I_n)^2$ and a variable step size duty cycle.

In an adaptive MPPT based on the INC concept [9], the scanning is performed by adjusting the duty cycle of the DC-DC converter used, and the search condition is to make the difference $V_r(n)-V(n)<\varepsilon$, where $V_r(n)$ is given by $I_{pv}(n)\times r_{pv}(n)$ and r_{pv} is the incremental dynamic resistance of the PV module and I_{pv} is PV module's current.

Similarly, in another adaptive MPPT based on the P&O concept [10], the scanning algorithm modifies the duty cycle dictated by $D=D\pm M\times dD$, where $M=(V_{n+1}-V_n)/(P_{n+1}-P_n)\times(P_n-P_{n-1})/(V_n-V_{n-1})$, and the search condition is similar to the P&O method.

There is an MPPT method suggested which depends on static conductance [11], where the search condition is to eliminate the error 'ε' between the internal reference power and the actual power, $\varepsilon=P_{ref}(t_n)-P_{pv}(t_n)$, from the PV module and the scanning is performed by modifying the input conductance of the DC-DC converter seen by the PV module.

There are available direct MPPT methods; in one such technique [12], under uniform irradiation, the search for MPP is done using the power balance equation $P_{ref}=P_{pv}+K\times dP/dV$ and the scanning pattern is controlled by the second term called power adjustment. In contrast, under partially shaded conditions, the method will behave as a conventional P&O.

In another direct MPPT method [13], the scanning algorithm depends on the charging profile of the input capacitor voltage 'V_c', and the search condition checks whether the slope of V_c^2, V_c and change in V_c the present and previous iterations are equal.

An MPPT technique based on a perturbation function is suggested [14] in literature, in which the scanning is carried out through adjusting the duty cycle by $D_{n+1}=D_n+\Delta D_n$, which ΔD_n is a complex function of the slope of the PV curve and its difference between two successive iterations in discrete form and the search condition is to make the difference in slope of the PV curve equal to zero. In another method [15], where scanning is based on modifying the duty cycle of the DC-DC Converter, the search condition is to detect the point at which the phase difference between the PV current and voltage starts to deviate.

Hybrid techniques combining conventional techniques are also available in the literature. In one of the methods [16], P&O is combined with the Fractional Short Circuit Current (FSCC) technique, where the scan and search procedure of P&O is deployed to track MPP; however, the launching point of P&O is decided by the FSCC.

Techniques of Global Maximum Power Point (GMPP) Tracking combining P&O with global search techniques have also been proposed by researchers. In one of the techniques [17], the global scanning is done around every peak of the PV curve in search for GMPP; however, in another technique [18], the global scanning is done only in the region that contains the GMPP through voltage sector technique, however the local scan and search in both the methods are done using P&O technique.

Further, in another such global MPPT technique, a marginal maximum power concept is used [19], where the search area is limited, in which the scanning is done to determine the location of different local peaks through the scan and search concept of P&O with larger step size and once the vicinity of GMPP is determined among the local peaks, P&O with smaller step size is used to track the GMPP.

In yet another method of GMPPT [20], two stages of scanning and search are used. In the first stage, linear scanning is performed to determine the global MPP. After determining the GMPP, the second stage is activated, wherein scanning is performed by changing the duty cycle in search of the PV array voltage to reach the V_{mpp} obtained in stage one. In another technique called the improved power increment-based MPPT technique [21], three lines, the voltage line, the current line, and the power line, are used to determine the MPP. In this method, scanning was also done by modulating the duty cycle.

A new technique called SOFT-MPPT, which is applicable to both P&O and INC, is suggested [22]. In this method the

scanning algorithm is based on an adaptive step size defined by $\Delta D_n=\Delta D_{min}+M_n\times \Delta P_n/\Delta V_n$ is used to determine the duty cycle for the next iteration, where M_n is inversely proportional to a fraction of I_n, whereas the search conditions are to check whether $|V_n-V_{n-2}|<\varepsilon$ and $V_{n-1}<V_n$.

In an MPPT technique proposed in literature based on the geometrical method [23], the scanning process is done by varying the duty cycle with different step sizes at different stages, and the two search conditions are to check for at every iteration whether i)ΔV_{pv} and ΔI_{pv} are zero and ii)$V_{pv}(n)(\Delta I_{pv}/\Delta V_{pv})+I_{pv}(n)$ and $V_{pv}(n)(\Delta V_{pv}/\Delta I_{pv})+I_{pv}(n)$ are zero.

In [24], Niraja et al. have suggested a Fixed Zone P&O technique in which the scanning is performed by modulating the duty cycle wherein the perturbation size is a combination of fixed and adaptive step sizes based on the zone in which the operating point lies and the search condition is similar to that of conventional P&O.

In another technique [25], the operating region is divided into different sectors, and the scanning is done by modulating the PV voltage based on the distance of the sector from the MPP and the search condition is similar to that of the conventional P&O. Hence, and it is obvious from many MPPT techniques for PV applications existing insofar, the scanning algorithms and search conditions play a crucial role in the determination of MPP. It is obvious from the MPP techniques presented that the process of scanning involved in the determination of MPP is a complex process, with many decisions made with more computational burden leading to overall complexity.

In this paper, a new method of MPPT with less decision-making and computational tasks is suggested. In the proposed techniques, a novel exponential scanning algorithm is introduced with a different approach to the favorable region of the PV curve with search conditions to achieve MPP faster under uniform irradiation. The scanning technique presented does not depend on any characteristic parameters for its search to find the MPP location but relies on very simple mathematical calculations.

2. Character of the PV Module and Defining the Power Zone

The non-linear mathematical model of the current vs voltage characteristic of a PV module is represented by the expression in (1).

$$I_{pv} = I_p - I_{os}\left\{\exp\left(\frac{V_{pv}+IN_sR_{se}}{nN_sV_T}\right)-1\right\}-\left(\frac{V_{pv}+IN_sR_{se}}{N_sR_{sh}}\right) \quad (1)$$

Where V_{pv} and I_{pv} are the PV Module's terminal voltage and current, respectively, the photo-generated current and reverse saturation current are represented by I_p and I_{os}, respectively, V_T is Volts Equivalent temperature, N_s is the number of PV cells connected in Series, R_{sh} and R_{se} represent the parasitic shunt and series resistances and n is the diode ideality factor of the PV cell.

The power vs voltage characteristic shall be obtained by multiplying (1) with V_{pv}, and its graphical illustration for different irradiation levels at two temperatures is shown in Figure 1. Studying the characteristic features of the PV characteristics, the P-V characteristic of the PV module shall be divided into three regions wherein the current and voltage are constant in two regions, and the power is significant in the remaining region [26].

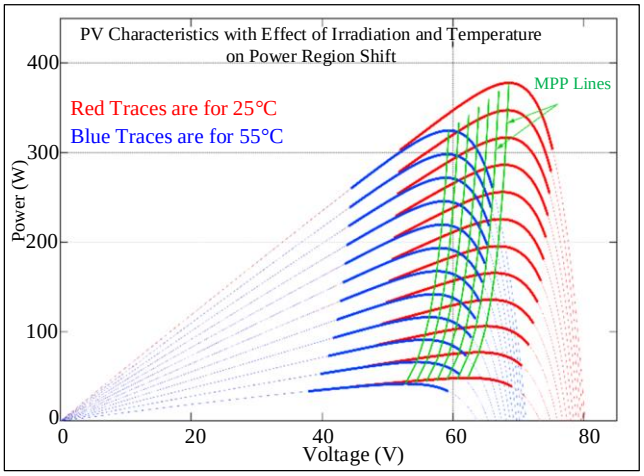

Fig. 1 P-V Characteristics with emphasis on power region

The power region of the P-V characteristic is defined in this paper as the portion of the characteristic wherein the power that the PV module can generate is greater than 80 percent of the maximum power to be delivered by the PV module at an individual environmental condition.

The graphical illustration of the power region of P-V characteristics for different environmental conditions is presented in Figure 1 by thick solid lines. From this figure, it is clear that the P-V curve is shifted upwards and away from the ordinate when the level of irradiation increases. When the temperature increases, the curve shifts towards the ordinate. The same trends are also applicable to the power region. The MPP lines for different environmental conditions are also illustrated in Figure 1, which follows the same shifting pattern described above for temperature.

The range of voltage that accommodates the power region is used as the voltage control space for implementing the MPPT presented in this paper. Due to the shifting nature of the power region, the voltage control space is defined to accommodate the entire range of temperature variation considered for implementation at a specific geographical location.

3. Proposed Method of MPPT

It is well known that the slope of the PV characteristic at MPP is zero, i.e., dP/dV=0. It can be represented equivalently in discrete form as given in (2) [3, 27].

$$Slope = \frac{dP}{dV} \equiv \frac{\Delta P}{\Delta V} = \frac{P_n - P_{n-1}}{V_n - V_{n-1}} = 0 \quad (2)$$

When the numerator approaches an infinitesimal degree, the slope approaches zero; however, under such circumstances, in the case of the PV characteristic, the difference V_n-V_{n-1} will also approach an infinitesimal value. Therefore, if the difference V_n-V_{n-1} is allowed to approach very smaller values such that if P_n-P_{n-1} approaches infinitesimally smaller value to make $\Delta P/\Delta V \rightarrow 0$, the MPP is approached.

In this paper, instead of taking an incremental value of ΔV, the difference V_n-V_{n-1} will be taken initially as a larger interval wherein a scanning algorithm is used to make the difference approaching smaller values with a search condition to satisfy (P_n-P_{n-1})→0, enabling to reach the MPP by achieving their ratio approaches to zero.

Also, in the proposed method, the power zone of the PV characteristic alone is considered for MPP tracking, and an interval is introduced in the power zone. The selection of such intervals will be explained later in section IV. In the defined interval, scanning in search of MPP is carried out successively so that a new operating interval is redefined with any one of the interval points updated.

The new operating interval point and the step size are derived and explained as follows:

Let the initial interval points be V_r and V_0, where V_r is a point of higher voltage, and V_0 is a point of lower voltage, then the first update of the interval point is, $V_1=(V_0+V_r)/2$ the second update of the interval point is $V_2=(V_1+V_r)/2$ and so on. The step size for the first update is $S_1=V_1-V_0=\frac{V_r}{2}-\frac{V_0}{2}$. The step sizes for the second and third updates are given below $S_2=V_2-V_1=\frac{V_r}{4}-\frac{V_0}{4}$, $S_3=V_3-V_2=\frac{V_r}{8}-\frac{V_0}{8}$.

Generally, the step size is given by,

$$S_n = \frac{V_r}{2^n} - \frac{V_0}{2^n} = \frac{1}{2^n}(V_r - V_o) \quad (3)$$

Where n > 0.

The update of the interval point is generally expressed by the expression in (4):

$$V_n = V_0 + \sum S_n = V_0 + \sum \frac{1}{2^n}(V_r - V_0) \quad (4)$$

Which can be written as in (5).

$$V_n = V_0\left(1 - \sum \frac{1}{2^n}\right) + V_r \sum \frac{1}{2^n} \quad (5)$$

In order to avoid the summations and to reduce the computational burden in (5), it can be equivalently expressed as (6).

$$V_n = \frac{V_0}{2^n} + V_r\left(1 - \frac{1}{2^n}\right) \quad (6)$$

Where n > 0 and $V_r > V_0$. This equation makes the voltage V_n approach V_r from V_0 at every iteration step.

When the variables in (6) satisfy the inequality $V_r > V_0$, $V_n \rightarrow V_r$ i.e., scanning from lower voltage to higher voltage happens, which is defined as forward scanning, whereas when they are interchanged, as given in (7), reverse scanning will occur $V_n \rightarrow V_0$.

$$V_n = \frac{V_r}{2^n} + V_0\left(1 - \frac{1}{2^n}\right) \quad (7)$$

While the iteration continues through forward scanning, the MPP will be crossed at one point during the interval step. Assuming that when the MPP is crossed in the n^{th} step, the voltage pertaining to the current step will be assigned as V_0 and that of the previous step, i.e. $(n-1)^{th}$ will be assigned as V_r, making reverse scanning take place. The above procedure is followed until both the interval points merge or are within the defined threshold.

Hence, interchanging the variables upon crossing the MPP will reverse the direction of scanning, ensuring the interval points approach together and finally reach MPP without any divergence. In selecting the interval, one of the interval points will be at a higher power level, whereas the other will be at a lower power level. V_r will initially be assigned to the voltage corresponding to a higher power level when the scanning starts.

Since the voltage V_n is inversely proportional to the exponent of 2, its value approaches the final value V_r in a faster manner, making the scanning process quicker. If the iteration step size needs to be decreased, then Equation (6) shall be modified into an expression as follows.

$$V_n = \frac{V_0}{2^{\frac{n}{m}}} + V_r\left(1 - \frac{1}{2^{\frac{n}{m}}}\right) \quad (8)$$

Where m shall be any real number greater than 1; however, using Equation (8), more steps are required to reach the MPP. The scanning profiles of (6), (8) and linear fixed step size increments for forward and reverse directions are illustrated in Figure 2. From Figure 2, it is obvious that the scanning done through the proposed method is faster in comparison with the fixed step size. During the scanning process, the new interval point will replace one of the previous

interval points subject to the following search condition given in (9).

$$P_n > P_{n-1} \rightarrow V_{n-1} = V_n \quad (9)$$

Also, the endpoint of the interval V_r will be replaced by the new interval point V_n subject to the condition in (10) only when the power corresponds to the new interval point is less than that of the previous interval point, i.e., $P_n < P_{n-1}$, indicating the crossing of the MPP. After replacing the endpoint, V_n becomes the start point, and V_{n-1} becomes the endpoint and the scanning direction changes. In this way, the forward and reverse scanning are performed. Every time when the scanning direction changes sequentially, the interval step sizes become self-adaptive numerically.

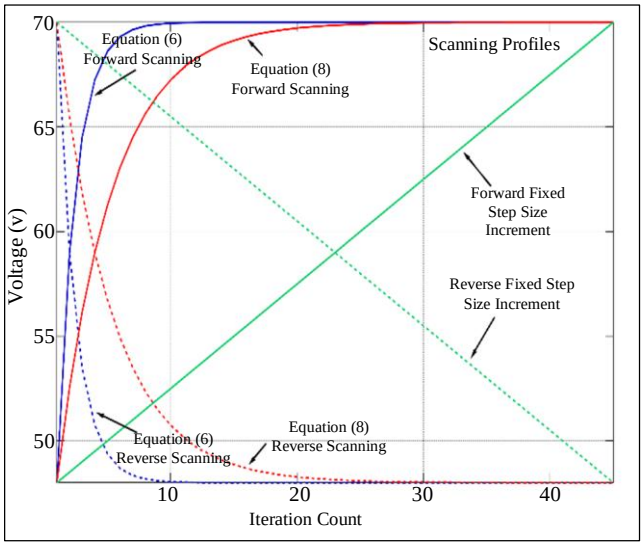

Fig. 2 Scanning profiles

$$P_n < P_{n-1} \rightarrow V_r = V_{n-1} \text{ and } V_0 = V_n \quad (10)$$

The scan and search actions will be stopped when the conditions given in (11) and (12) are met, describing the voltage and power difference between the current iteration and the previous iteration.

$$|\Delta V_n| = |V_n - V_{n-1}| \leq \varepsilon_v \quad (11)$$

$$|\Delta P_n| = |P_n - P_{n-1}| \leq \varepsilon_p \quad (12)$$

Where ε_v and ε_p are user-defined threshold limits for voltage and power differences.

After reaching the MPP, any change in irradiation is monitored by measuring the change in power ΔP_n periodically. If the ΔP_n is greater than a power threshold corresponding to a lesser change in the irradiation level, a new narrow voltage interval is defined, and the entire tracking process is reinitiated. Otherwise, another wide voltage interval is defined, and the tracking is reinitiated. The concept of such a user-defined choice of intervals is shown in Figure 3. The implementation of the proposed method of MPPT, as stated above, is illustrated in Figure 4 in the form of a flow chart.

4. Selection of Interval

Practically, it is difficult to determine the endpoints as stated above without conducting an experiment at standard test conditions to know the power zone. This paper suggests the following method is used to determine the initial interval endpoints practically in consultation with the data provided in the datasheet by the PV module's manufacturer.

1. The endpoint on the Constant Voltage (CV) region V_{cv} shall be determined with reference to the V_{mpp} and V_{oc} at STC, and these data are provided in the PV module's datasheet. The expression to determine V_{cv} is given by:

$$V_{mpp-STC} < V_{cv} \leq V_{oc-STC} - 0.75(V_{oc-STC} - V_{mpp-STC}) \quad (13)$$

2. The other endpoint on the Constant Current (CC) region V_{cc} shall be determined with reference to the V_{mpp} at STC and V_{TD}, and these data shall also be indicated in the PV module's datasheet. The expressions to determine V_{cc} are given as follows.

$$V_{cc} \geq 0.75 V_{mpp\text{-}STC} - V_{TD} \quad (14)$$

$$V_{TD} = N_m \alpha_{V_{oc}} \Delta T \quad (15)$$

Where V_{TD} represents the thermal drift in V_{oc}, N_m is the number of modules connected in series, $\alpha_{V_{oc}}$ is the temperature coefficient of V_{oc} in V/°C, and ΔT is the difference in temperature between the STC and the maximum operating temperature considered. Such selection places the endpoints in the CV and CC regions on the power region.

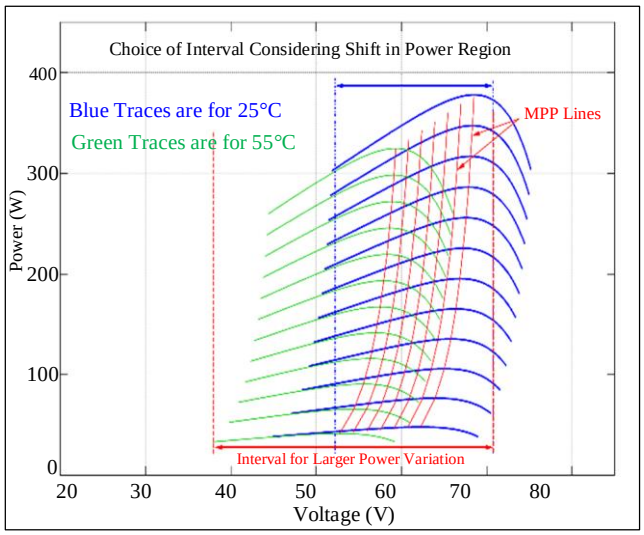

Fig. 3 Choice of interval

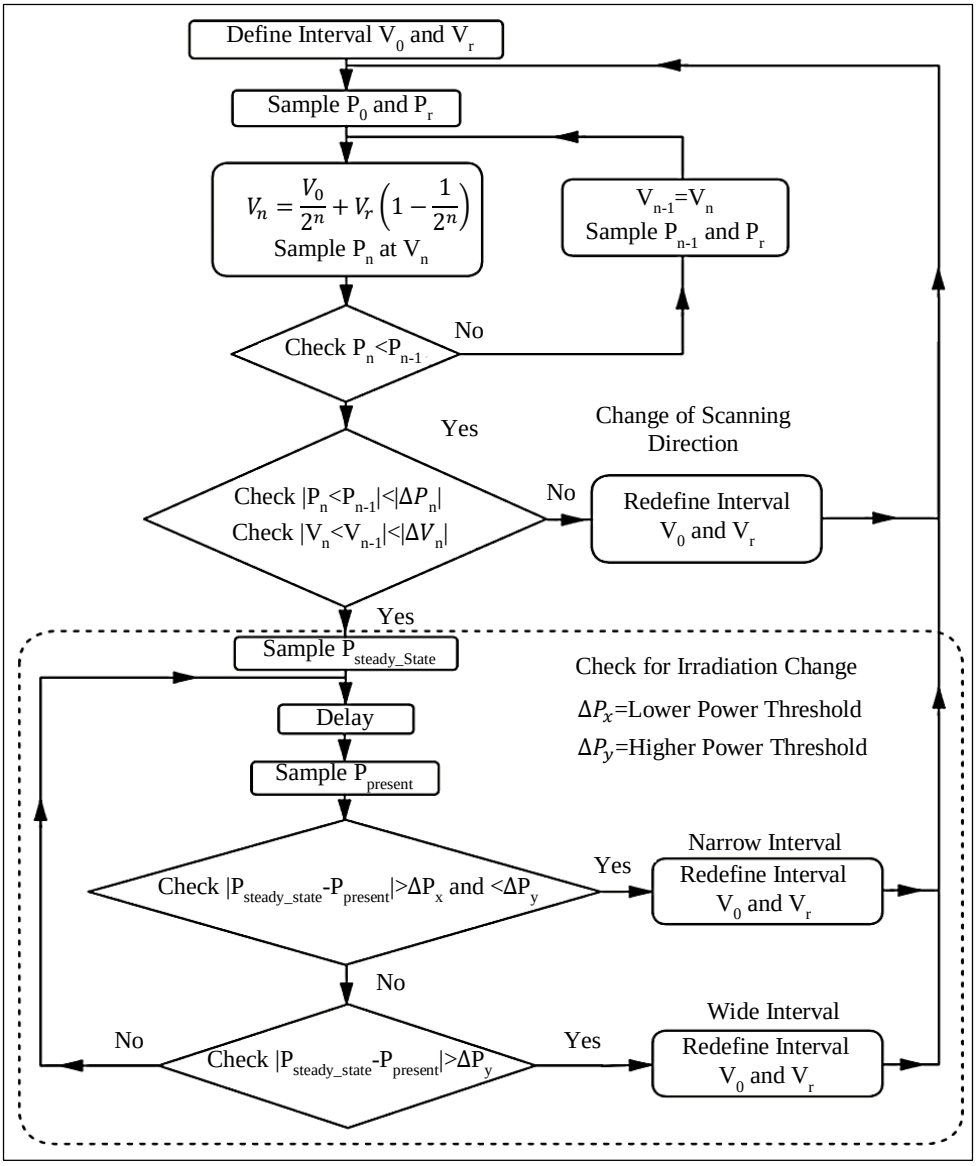

Fig. 4 Flowchart of the proposed technique

5. Evaluation through Computer Simulation

The proposed method is verified through computer simulations using PLECS software, wherein the evaluation is done with the help of a Buck converter interposed between a PV array and a Battery load. The evaluation is carried out using many irradiation patterns, and for the sake of brevity, the following two patterns of irradiation and temperature are presented.

- Static condition - 1000 W/m^2 @ 35^{o}C
- Dynamic condition comprising the following sequence - a) 900 W/m^2 @ 35^{o}C for 1.5 seconds, b) 885 W/m^2 @ 35^{o}C for 1.5 seconds, c) 200 W/m^2 @ 35^{o}C for 1.5 seconds, d) Temperature increased to 45^{o}C @ 4.45 seconds, e) 700 W/m^2 @ 45^{o}C for 1.5 second and f) 400 W/m^2 @ 35^{o}C.

The transient response and the convergence process under static conditions are illustrated in Figure 5 and Figure 6, respectively, which clearly show the step-by-step process of computing the operating points iteratively in a sequential manner, the effectiveness of tracking and the successful convergence of the proposed method towards MPP in a fast manner without any divergence. The time behavior under dynamic conditions is illustrated in Figure 7, wherein the power extracted after reaching every steady state is also indicated. In the first transition of the dynamic condition, i.e., from pattern 2(a) to 2(b), a narrow voltage control interval for smaller power variation is invoked by the algorithm as the change in power level is within the threshold level, whereas at all other transitions, a wide voltage control interval for larger power variation is invoked as the change in power level is above the threshold.

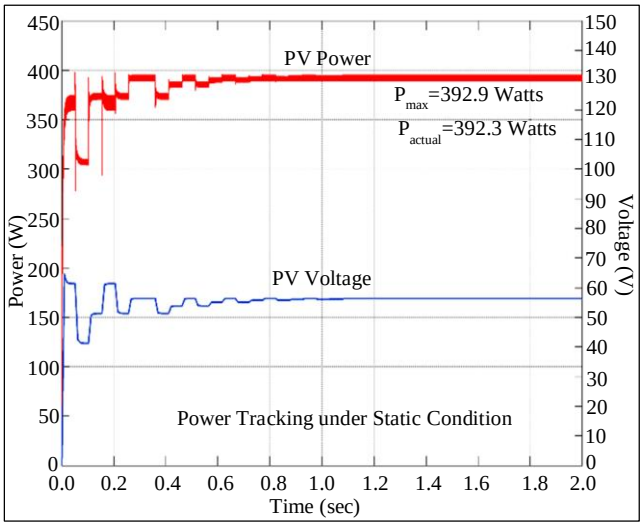

Fig. 5 Transient response under static condition

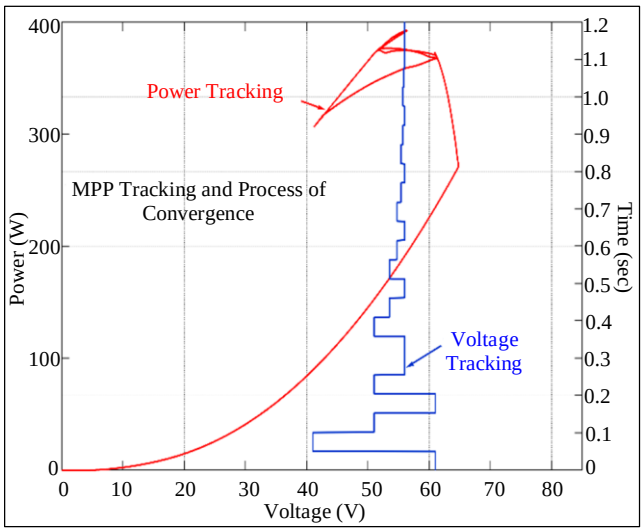

Fig. 6 Convergence process of the proposed technique

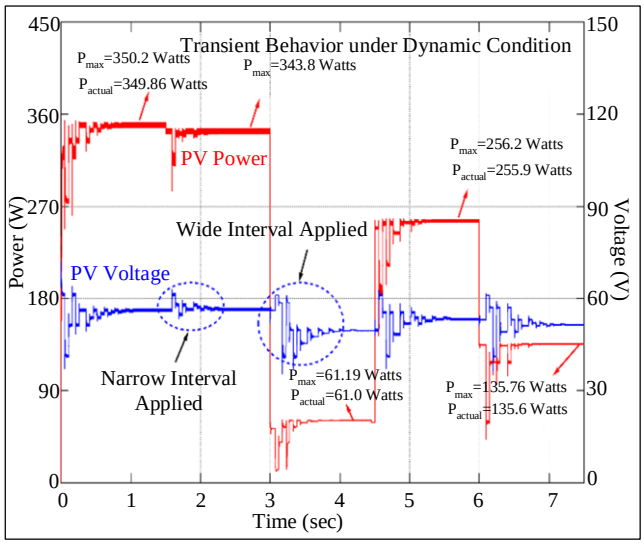

Fig. 7 Transient response under dynamic condition

Under dynamic conditions, the response produced is quite encouraging. It is also observed from the transient response for dynamic conditions that the tracking time is decreased when a narrow interval is invoked for a smaller power change than for a wider interval for a larger power change.

6. Experimental Evaluation

In order to verify the proposed method experimentally, a buck converter is fabricated with the same value of components used for simulation and operated at 20kHz. The designed buck converter with the functional block diagram for experimental verification is shown in Figure 8.

The PV array used comprises of 4 numbers of 125-watt PV modules, all connected in series mode. Three numbers of 12V batteries in series connected mode are used as a load to store the energy extracted. The proposed technique is implemented through a low-cost dsPIC30F2010 digital signal controller, which produces a 20kHz PWM signal whose duty cycle is indirectly controlled by a digital PI controller.

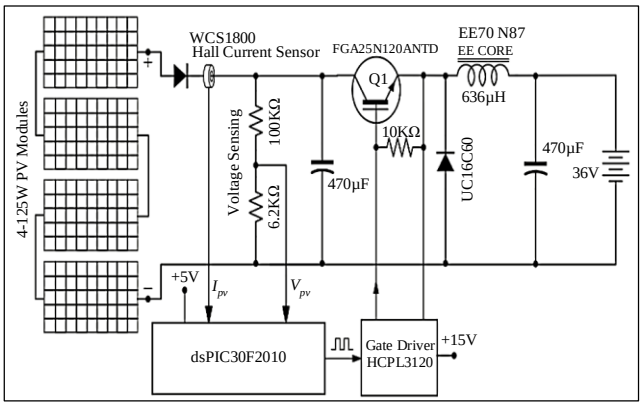

Fig. 8 Functional Schematic diagram for experimental verification

Experiments are conducted under two natural environmental conditions: i) a static condition and ii) a dynamic condition. The temperature, irradiation level, and wind velocity at the time of experimenting are constant, consistent, and uniform, and they do not affect or influence the performance of the techniques used. The data are acquired with the help of a Tektronics oscilloscope, and the maximum power obtained is compared with that obtained by a solar array analyzer from MECO. Another oscilloscope from Keysight is used to monitor the activity of the proposed MPPT while it is under operation. In the experimental study, all measurements are carried out at the input terminals of the buck converter.

The response obtained for a static condition is illustrated in Figure 9, where the response pattern agrees well with the response obtained through computer simulation for static conditions by the PLECS software. At this condition, the maximum power extracted by the proposed technique at steady state is 380 watts, and the actual maximum power from the PV array at the input terminals of the buck converter is

380.6 watts, measured with the help of the Solar Array Analyzer. The photograph snapshot of the front panel of the Solar Array Analyzer is shown in Figure 10.

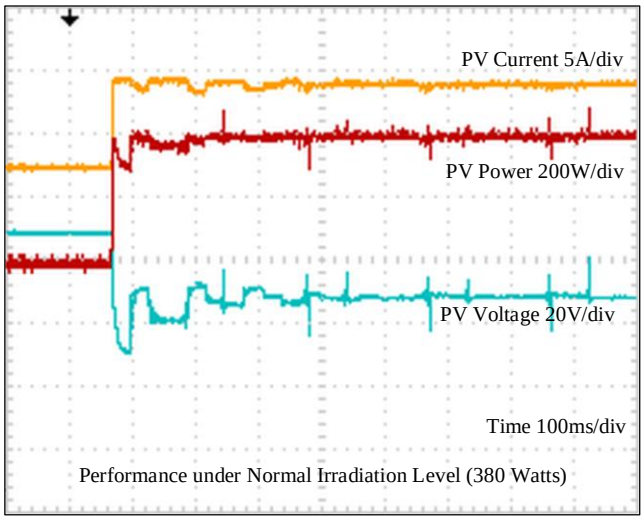

Fig. 9 Experimental response under a normal power level

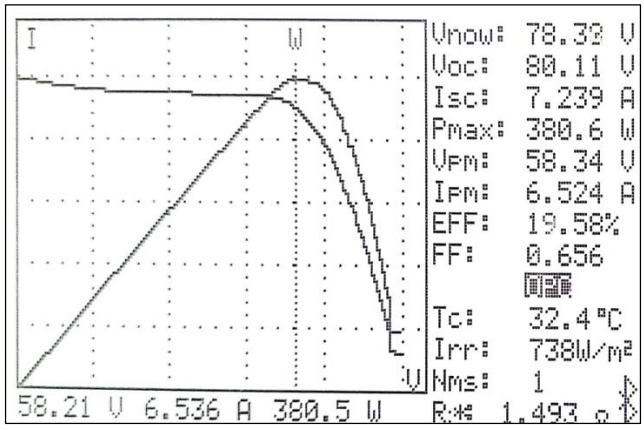

Fig. 10 Solar analyzer front panel snapshot for Figure 9

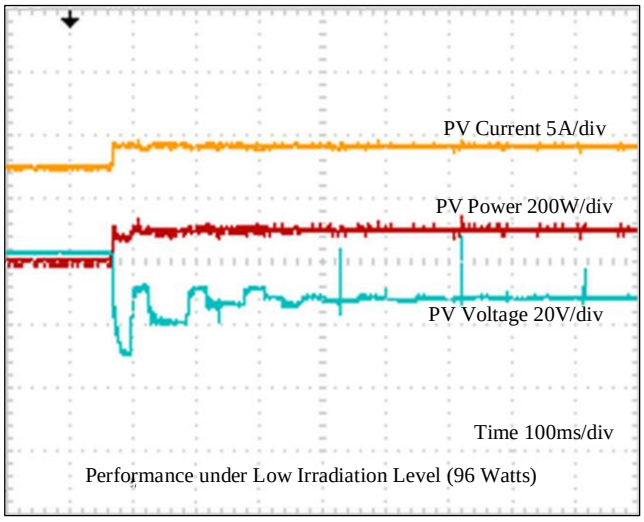

Fig. 11 Experimental response under a low power level

The performance obtained under a low irradiation level is illustrated in Figure 11, wherein the power extracted is 96 watts, and the maximum power measured with the Solar Array Analyzer is also 96 watts, giving an excellent efficiency. The front panel snapshot of the Solar Array Analyzer is shown in Figure 12.

Also, the behavior of the proposed technique under a natural slow varying dynamic condition is carried out, whose response is illustrated in Figure 13, wherein it is clear that the power from the PV array is gradually decreasing after reaching the first steady state condition in the startup instance. The algorithm is reinitiated in two instances after that when the power level is reduced and within the threshold limit.

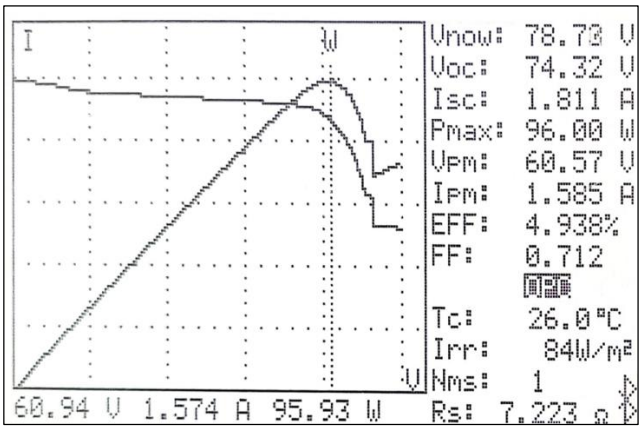

Fig. 12 Solar analyzer front panel snapshot for Figure 11

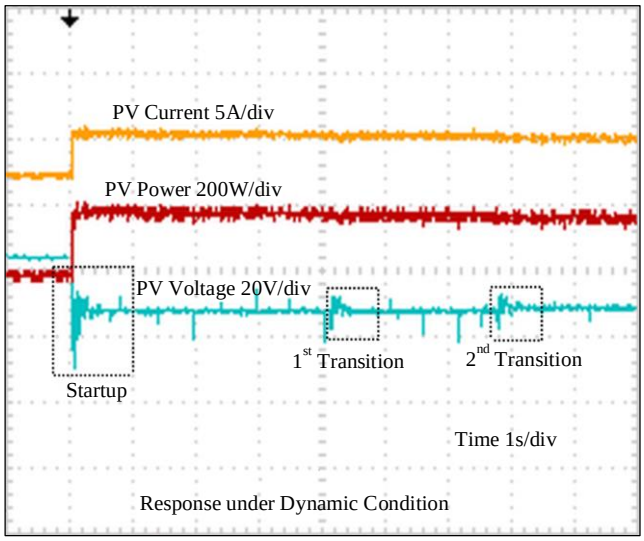

Fig. 13 Performance under a dynamic condition

It is also clear from Figure 13 that the voltage is updated in the second transition; however, it is not perceptible in the first transition as the maximum power point voltage is very close to that of the steady state voltage after startup. Further, the voltage interval in the first and the second transitions is narrower than at startup. This is due to the fact that the

decrease in the power level is within the designed threshold limit corresponding to the narrow interval, as explained in the flow chart of Figure 4.

Also, a comparative analysis of the proposed techniques is performed using popular techniques such as Perturb observation and incremental conductance. The final efficiency at a steady state and the time to reach the peak power point are the indices for comparison. The performance comparison is reported in Table 1. The measurement of efficiency is computed from the data captured through the DSO. The selection of data from the DSO capture to calculate the efficiency is those data after attaining a steady state.

Table 1. Performance comparison

Parameter	Proposed	P&O	INC
Average Efficiency	99.8%	99%	99.2%
Time	632 milli-sec	850 milli-sec	770 milli-sec

7. Results and Discussion

The response of the proposed MPPT, assessed through computer simulation and experimental study, shows the quality of congruence with the algorithm presented in section 3 and the flowchart in Figure 4. Further, the transient responses observed in the experimental studies are well in agreement with the computer simulations, which indicates the success of the proposed technique. Moreover, the efficiency produced by the proposed technique under static environmental conditions through simulation is 99.8%, and the same measured through experimental evaluation is also 99.8%. These efficiencies show that there is an excellent agreement between simulation study and experimental study.

Also, the similarity in the responses produced through simulation and experiment under dynamic conditions exhibits the excellent convergence behavior of the proposed technique with a faster convergence time of less than 632 mill-second. Though the algorithmic convergence is 632 milli-seconds, the measurement through a digital storage oscilloscope reveals that the proposed method has reached very close to the MPP in almost 330 milli-seconds, which is a good phenomenon in improving energy extraction efficiency. Moreover, it is obvious that the tracking time is still reduced by reducing the width of the interval, which is applied under reduced change in power levels.

From the comparison of the performance of the proposed technique with P&O and INC, it is obvious that the performance of the proposed technique is far better in terms of final efficiency and the time it takes to reach MPP. Finally, though it cannot be stated as a limitation, one of the conditions at the point of implementation is that the threshold limits for the change in voltage and the change in power should not be too small as it would take a longer time to settle. Also, as a future work, this technique shall be extended for the partially shaded conditions of PV modules if the voltage range for the potential regions in which the GMPP is identified.

Thus, the presented MPPT technique in this paper has an excellent performance with tracking efficiency, is generic in nature and depends on the PV module's parameter presented in the data sheet with less computational effort; further, its cost of implementation is also less given a positive attribute to the proposed technique.

8. Conclusion

A new technique of MPPT with sequential self-adaptive scanning is presented in this paper. The process involved in the technique requires the data of the PV module, which are provided by the manufacturer in the data sheet. The computational efforts required for implementation are less; hence, a low-cost digital signal processor or a microcontroller can be used. The practical selection of the interval depending on the change in power level due to a change in irradiation is presented, which can be obtained easily.

The presented technique is evaluated through computer simulation using PLECS software and experimentally verified. The responses obtained through simulations and experimental studies are matched excellently. The efficiency of tracking obtained through simulation and experimentation is well agreed upon and encouraging. The convergence of the proposed method of MPPT under static and dynamic environmental conditions is fast, and the steady state performance is appealing. The practical implementation is done with a dsPIC30F2010 digital signal controller, allowing the complete work to be finished successfully at a low cost.

References

[1] Unchittha Prasatsap et al., "Comparison of Control Configurations and MPPT Algorithms for Single-Phase Grid-Connected Photovoltaic Inverter," *Advances in Electrical and Computer Engineering*, vol. 23, no. 2, pp. 55-66, 2023. [CrossRef] [Google Scholar] [Publisher Link]

[2] Dezso Sera et al., "On the Perturb-and-Observe and Incremental Conductance MPPT Methods for PV Systems," *IEEE Journal of Photovoltaics*, vol. 3, no. 3, pp. 1070-1078, 2013. [CrossRef] [Google Scholar] [Publisher Link]

[3] Sergei Kolesnik, and Alon Kuperman, "On the Equivalence of Major Variable-Step-Size MPPT Algorithms," *IEEE Journal of Photovoltaics*, vol. 6, no. 2, pp. 590-594, 2016. [CrossRef] [Google Scholar] [Publisher Link]

[4] Salah Necaibia et al., "Enhanced Auto-Scaling Incremental Conductance MPPT Method, Implemented on Low-Cost Microcontroller and SEPIC Converter," *Solar Energy*, vol. 180, pp. 152-168, 2019. [CrossRef] [Google Scholar] [Publisher Link]

[5] Hafsa Abouadane et al., "Multiple-Power-Sample Based P&O MPPT for Fast-Changing Irradiance Conditions for a Simple Implementation," *IEEE Journal of Photovoltaics*, vol. 10, no. 5, pp. 1481-1488, 2020. [CrossRef] [Google Scholar] [Publisher Link]

[6] Gautam A. Raiker, Umanand Loganathan, and Subba Reddy B., "Current Control of Boost Converter for PV Interface with Momentum-Based Perturb and Observe MPPT," *IEEE Transactions on Industry Applications*, vol. 57, no. 4, pp. 4071-4079, 2021. [CrossRef] [Google Scholar] [Publisher Link]

[7] V. Jately, and S. Arora, "Development of a Dual-Tracking Technique for Extracting Maximum Power from PV Systems under Rapidly Changing Environmental Conditions," *Energy*, vol. 133, pp. 557-571, 2017. [CrossRef] [Google Scholar] [Publisher Link]

[8] Ankit Kumar Soni, Kartick Chandra Jana, and Deepak Kumar Gupta, "Variable Step-Size Adaptive Maximum Power Point Tracking Algorithm for Solar Cell under Partial Shading Conditions," *IETE Journal of Research*, vol. 69, no. 3, pp. 1562-1577, 2023. [CrossRef] [Google Scholar] [Publisher Link]

[9] Bidyadhar Subudhi, and Raseswari Pradhan, "A New Adaptive Maximum Power Point Controller for a Photovoltaic System," *IEEE Transactions on Sustainable Energy*, vol. 10, no. 4, pp. 1625-1632, 2019. [CrossRef] [Google Scholar] [Publisher Link]

[10] Premkumar Manoharan et al., "Improved Perturb and Observation Maximum Power Point Tracking Technique for Solar Photovoltaic Power Generation Systems," *IEEE Systems Journal*, vol. 15, no. 2, pp. 3024-3035, 2021. [CrossRef] [Google Scholar] [Publisher Link]

[11] Oswaldo Lopez-Santos et al., "Analysis, Design, and Implementation of a Static Conductance-Based MPPT Method," *IEEE Transactions on Power Electronics*, vol. 34, no. 2, pp. 1960-1979, 2019. [CrossRef] [Google Scholar] [Publisher Link]

[12] Faicel El Aamri et al., "A Direct Maximum Power Point Tracking Method for Single-Phase Grid-Connected PV Inverters," *IEEE Transactions on Power Electronics*, vol. 33, no. 10, pp. 8961-8971, 2018. [CrossRef] [Google Scholar] [Publisher Link]

[13] Enrico Dallago et al., "Direct MPPT Algorithm for PV Sources with only Voltage Measurements," *IEEE Transactions on Power Electronics*, vol. 30, no. 12, pp. 6742-6750, 2015. [CrossRef] [Google Scholar] [Publisher Link]

[14] S.M. Reza Tousi et al., "A Function-Based Maximum Power Point Tracking Method for Photovoltaic Systems," *IEEE Transactions on Power Electronics*, vol. 31, no. 3, pp. 2120-2128, 2016. [CrossRef] [Google Scholar] [Publisher Link]

[15] Chin-Sien Moo, and Gwo-Bin Wu, "Maximum Power Point Tracking with Ripple Current Orientation for Photovoltaic Applications," *IEEE Journal of Emerging and Selected Topics in Power Electronics*, vol. 2, no. 4, pp. 842-848, 2014. [CrossRef] [Google Scholar] [Publisher Link]

[16] Hadeed Ahmed Sher et al., "A New Sensorless Hybrid MPPT Algorithm Based on Fractional Short-Circuit Current Measurement and P&O MPPT," *IEEE Transactions on Sustainable Energy*, vol. 6, no. 4, pp. 1426-1434, 2015. [CrossRef] [Google Scholar] [Publisher Link]

[17] Kai Chen et al., "An Improved MPPT Controller for Photovoltaic System under Partial Shading Condition," *IEEE Transactions on Sustainable Energy*, vol. 5, no. 3, pp. 978-985, 2014. [CrossRef] [Google Scholar] [Publisher Link]

[18] R. Balasankar, G. Tholkappia Arasu, and J.S. Christy Mano Raj, "A Global MPPT Technique Invoking Partitioned Estimation and Strategic Deployment of P&O to Tackle Partial Shading Conditions," *Solar Energy*, vol. 143, pp. 73-85, 2017. [CrossRef] [Google Scholar] [Publisher Link]

[19] Mohamad Amin Ghasemi, Hossein Mohammadian Foroushani, and Frede Blaabjerg, "Marginal Power-Based Maximum Power Point Tracking Control of Photovoltaic System under Partially Shaded Condition," *IEEE Transactions on Power Electronics*, vol. 35, no. 6, pp. 5860-5872, 2020. [CrossRef] [Google Scholar] [Publisher Link]

[20] K.S. Parlak, "A New High Performance MPPT Method Using only DC-DC Converter in Partial Shade Conditions," *Advances in Electrical and Computer Engineering*, vol. 23, no. 3, pp. 75-84, 2023. [CrossRef] [Google Scholar] [Publisher Link]

[21] Xingshuo Li et al., "A Novel Power-Increment Based GMPPT Algorithm for PV Arrays under Partial Shading Conditions," *Solar Energy*, vol. 169, pp. 353-361, 2018. [CrossRef] [Google Scholar] [Publisher Link]

[22] Shamik Bhattacharyya et al., "Steady Output and Fast Tracking MPPT (SOFT-MPPT) for P&O and InC Algorithms," *IEEE Transactions on Sustainable Energy*, vol. 12, no. 1, pp. 293-302, 2021. [CrossRef] [Google Scholar] [Publisher Link]

[23] Hassan Fathabadi, "Novel Fast Dynamic MPPT (Maximum Power Point Tracking) Technique with the Capability of Very High Accurate Power Tracking," *Energy*, vol. 94, pp. 466-475, 2016. [CrossRef] [Google Scholar] [Publisher Link]

[24] Niraja Swaminathan, N. Lakshminarasamma, and Yue Cao, "A Fixed Zone Perturb and Observe MPPT Technique for a Standalone Distributed PV System," *IEEE Journal of Emerging and Selected Topics in Power Electronics*, vol. 10, no. 1, pp. 361-374, 2022. [CrossRef] [Google Scholar] [Publisher Link]

[25] Ahmed I.M. Ali, Mahmoud A. Sayed, and Essam E.M. Mohamed., "Modified Efficient Perturb and Observe Maximum Power Point Tracking Technique for Grid-Tied PV System," *International Journal of Electrical Power & Energy Systems*, vol. 99, pp. 192-202, 2018. [CrossRef] [Google Scholar] [Publisher Link]

[26] J.S. Christy Mano Raj, and A. Ebenezer Jeyakumar, "A Novel Maximum Power Point Tracking Technique for Photovoltaic Module Based on Power Plane Analysis of I-V Characteristics," *IEEE Transactions on Industrial Electronics*, vol. 61, no. 9, pp. 4734-4745, 2014. [CrossRef] [Google Scholar] [Publisher Link]

[27] Qiyu Li et al., "An Improved Perturbation and Observation Maximum Power Point Tracking Algorithm Based on a PV Module Four-Parameter Model for Higher Efficiency," *Applied Energy*, vol. 195, pp. 523-537, 2017. [CrossRef] [Google Scholar] [Publisher Link]